

Recent Results

Generation of gauge configurations with the improved Asqtad action: We have nearly completed our long term project of generating gauge configurations with three flavors of improved Asqtad quarks. We have worked with a one-loop Symanzik improved gauge action and the Asqtad staggered quark action [1]. Both the gauge and quark actions have all lattice artifacts removed through order a^2 (a is the lattice spacing) at the tree level, and are tadpole improved. So, the leading discretization errors are of order $a^2/\log(a)$. The masses of the up and down quarks were taken to be equal, which has a negligible effect ($< 1\%$) on isospin-averaged quantities. The average value of the up and down quark masses, which we denote by m_l , is much smaller than other energy scales in QCD, and up to now it has been too expensive to perform simulations at its physical value. Instead, we have worked with a range of values for m_l which are small enough so that extrapolations to its physical value could be performed with the aid of chiral perturbation theory [2]. On the other hand, the strange quark mass is heavy enough so that we were able to perform simulations at its physical value m_s , and in most ensembles we attempt to keep it fixed at that value as we varied the lattice spacing and m_l .

We have generated Asqtad ensembles with lattice spacings $a \approx 0.18, 0.15, 0.12, 0.09$ and 0.06 fm with the light quark mass in the range $0.1 m_s \leq m_l \leq m_s$ and the strange quark mass fixed close to its physical value. We have also completed ensembles with $a \approx 0.045$ fm and $m_l = 0.2 m_s$ and $a \approx 0.09$ fm and $m_l = 0.05 m_s$. In addition, we have generated a number of ensembles with the strange quark mass less than its physical value to aid in chiral extrapolations. All of the Asqtad configurations are publicly available. A table of ensembles with $a \leq 0.12$ fm can be found at the link [asqtad configurations](#).

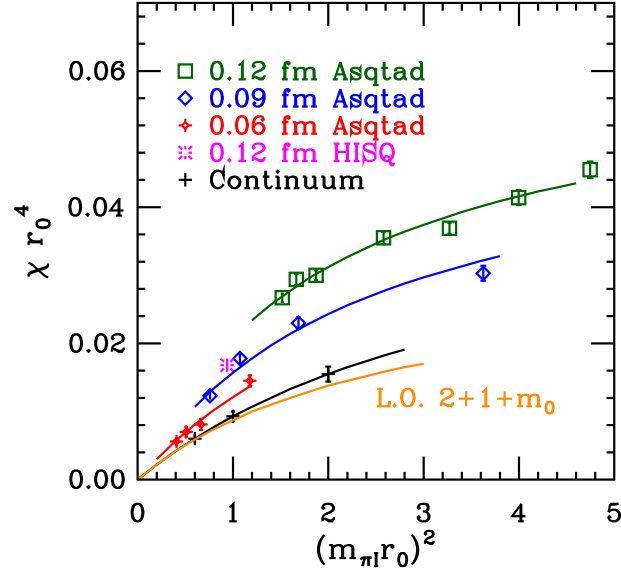


Figure 1: Comparison of the topological susceptibility for the Asqtad and HISQ actions. The colored plotting symbols are data points from our simulations, and the solid curves are from a chiral perturbation theory fit to all of the Asqtad data. The black curve and plotting symbols are extrapolations to the continuum limit. The yellow line is a leading order continuum χ PT calculation.

Generation of gauge configurations with the highly improved HISQ action: Our program of QCD simulations has now reached the point where moving to a more highly improved fermion

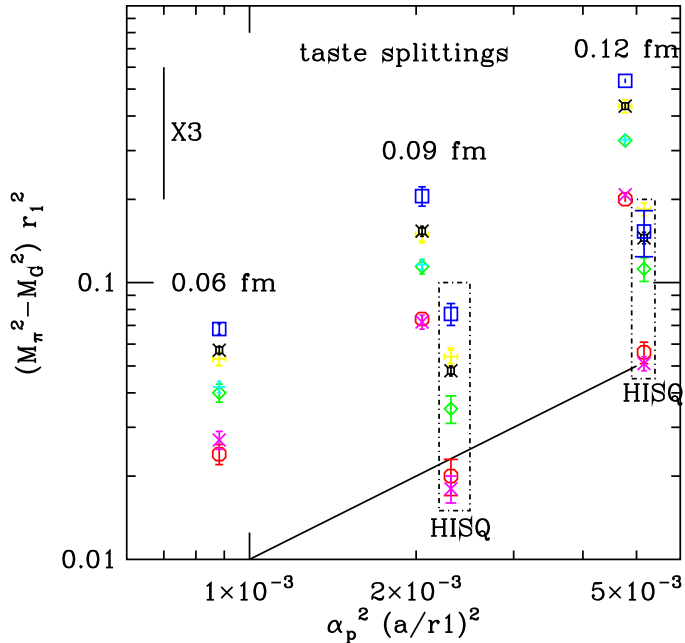


Figure 2: A comparison of taste splittings of the pion masses for the HISQ and Asqtad actions. The HISQ results are inside the dashed boxes. M_G is the mass of the Goldstone pion and M_π of one of the heavier pions. The abscissa is proportional to $a^2/\log(a)^2$. The line on the lower right illustrates the expected linear dependence of the mass splittings on the lattice spacing. The vertical bar labeled X3 shows the size of a factor of three on this log-log plot.

action is more efficient than further decreasing the quark mass and lattice spacing with the Asqtad action. The HISQ action, which was introduced by the HPQCD/UKQCD collaboration [3], is intended to reduce lattice artifacts while maintaining the economy of staggered quarks. Like the Asqtad action, the leading discretization errors for the HISQ action are of order $a^2/\log(a)$. However, the HISQ action has two important advantages over Asqtad. First, the HISQ action reduces taste symmetry violations significantly below those for the Asqtad action. Since taste symmetry violation effects are one of, if not the largest impediment to reducing errors in lattice QCD calculations with staggered quarks, the HISQ action provides a very promising path to improved accuracy. Furthermore, the HISQ action incorporates improvements in the quark dispersion relations that enable one to use it to describe charm quarks at lattice spacings accessible with today's computers, which is not the case for the Asqtad action.

We have begun to generate gauge configurations with four flavors of HISQ quarks: up, down, strange and charm. The strange and charm quarks are set close to their physical values, and, as in the case of the Asqtad ensembles the up and down quarks are taken to be degenerate. In the simulations undertaken to date, the light quark mass $m_l = 0.2m_s$, and ensembles are being generated with lattice spacings $a \approx 0.15, 0.12$ and 0.09 fm. In general, we find that a HISQ ensemble with lattice spacing a has lattice artifacts approximately the size of an Asqtad ensemble with lattice spacing $\frac{2}{3}a$. As an example, we show in Fig. 1 the topological susceptibility as a function of the taste singlet pion mass $m_{\pi l}$. Data is shown for the Asqtad action with three different lattice spacings. Note that the single HISQ point at lattice spacing $a \approx 0.12$ fm falls very close to the Asqtad curve for $a \approx 0.09$ fm. For the Asqtad action, the lattice artifacts for $a \approx 0.09$ fm are approximately half those at $a \approx 0.12$ fm. Similar results are obtained for a number of other physical quantities.

Taste symmetry violation effects show up most prominently in the splitting of the pions. In our full QCD calculations, we find that these splittings are reduced by a factor of approximately three

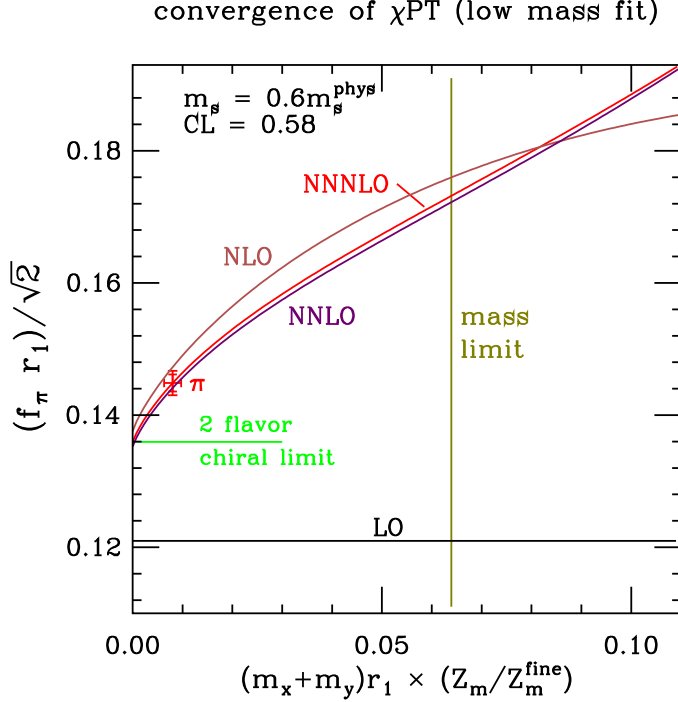


Figure 3: Contributions of each order in $SU(3)$ χ PT are shown for the pion decay constant, coming from a fit to our low-mass data. The leading order term is labeled “LO;” contributions from leading order and next-to-leading order are labeled “NLO,” *etc.* Here the simulated strange sea quark mass m'_s is always less than or equal to $0.6m_s$ (where m_s is the physical mass) and the valence masses obey $m_x + m_y \leq 0.6m_s$. At higher masses, near m_s , $SU(3)$ χ PT is less well behaved. But that is not a problem for us because we can fix the LO and NLO terms from a fit like this one, which then gives good control over the needed chiral extrapolation to low masses (the physical masses of the u and d quarks).

compared to those for the Asqtad action, as is shown in Fig. 2. Note that the vertical bar labeled X3 shows the size of a factor of three on this log-log plot.

During the coming year we plan to complete the three ensembles currently in progress with $m_l = 0.2m_s$, and generate additional ones with light quark masses $m_l = 0.1m_s$ and $0.04m_s$ using the same three lattice spacings. In the future we hope to generate ensembles at these three light quark masses and lattice spacings $a \approx 0.06$ fm.

Properties of light pseudoscalar mesons: During the past year we have extended our work on light pseudoscalar mesons to new ensembles with lattice spacings $a \approx 0.06$ and 0.045 fm, and to ensembles with the simulation strange quark mass m'_s less than the physical strange quark mass m_s . The latter ensembles are important because the physical strange quark mass is not light enough for $SU(3)$ chiral perturbation theory to converge rapidly in its vicinity. To anchor chiral fits and to test the convergence of chiral perturbation theory, it is therefore extremely helpful to have ensembles with the strange sea quark mass held fixed at a value well below the physical strange quark mass. Another improvement in the analysis is to consider fits to $SU(2)$ $S\chi$ PT in addition to our standard fits to $SU(3)$. The $SU(2)$ fits are likely to be a good approximation for ensembles with $m'_s = m_s$ and $m_l \ll m_s$; while $SU(3)$ should work best for $m'_s < m_s$. We find consistent physical results from both approaches. Figure 3 shows the good convergence of $SU(3)$ χ PT for $m'_s \leq 0.6m_s$, and the agreement with $SU(2)$ χ PT in the limit of vanishing light quark mass.

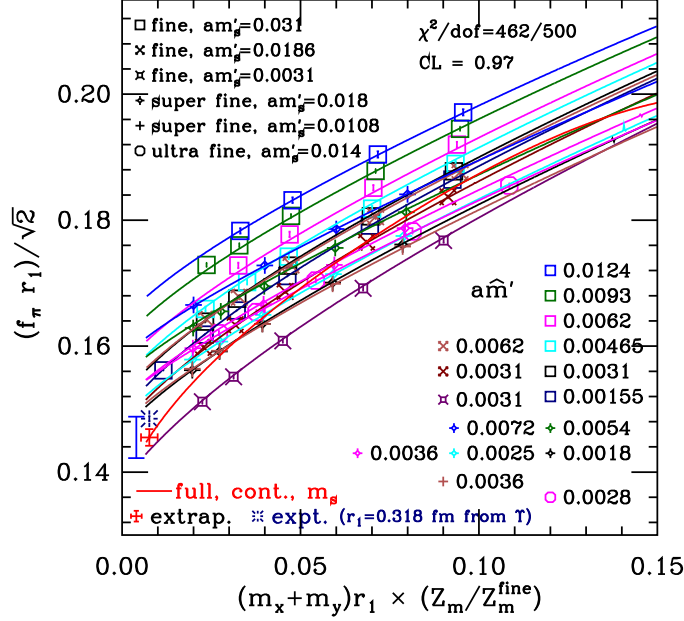


Figure 4: Pion decay constants vs. valence quark mass, in units of the scale r_1 . An $SU(3)$ chiral fit line for each ensemble is shown as a function of valence quark mass. Only “pion” points (two equal valence masses) are shown, although the fit-parameters of the lines come from the fit to the entire data set for decay constants and masses. The red line represents the result in full QCD after extrapolation of parameters to the continuum, and with strange sea quark fixed at its physical mass. The red plus shows our extrapolated value of f_π , in agreement with experiment (dark blue burst) within systematic errors (blue bar).

Preliminary results from the new analysis for f_π are:

$$SU(3): \quad f_\pi = 128.0 \pm 0.3 \pm 2.9 \text{ MeV} \quad SU(2): \quad f_\pi = 128.7 \pm 0.9 \pm_{-2.7}^{3.2} \text{ MeV} \quad (1)$$

using the $SU(3)$ and $SU(2)$ chiral fits, respectively. The first error is statistical and the second systematic. Our result for f_π is consistent with the experimental value [4] $130.4 \pm 0.2 \text{ MeV}$. The $SU(3)$ fit is shown in Fig. 4.

For other quantities, smaller systematic errors can be obtained by using f_π itself to set the lattice scale. We obtain

$$\begin{aligned}
f_K &= 156.2(3)(11) \text{ MeV} & |V_{us}| &= 0.2247(_{-13}^{+16}) \\
f_K/f_\pi &= 1.198(2)(_{-8}^{+6}) & \langle \bar{u}u \rangle_2 &= -(279(1)(2)(4) \text{ MeV})^3 \\
f_2 &= 122.8(3)(5) \text{ MeV} & \langle \bar{u}u \rangle_3 &= -(245(5)(4)(4) \text{ MeV})^3 \\
f_3 &= 111(2)(4) \text{ MeV} & \langle \bar{u}u \rangle_2 / \langle \bar{u}u \rangle_3 &= 1.47(1)(10) \\
f_2/f_3 &= 1.107(3)(39) & 2L_8 - L_5 &= -0.47(8)(14) \\
2L_6 - L_4 &= 0.19(12)(1) & L_5 &= 1.64(12)(17) \\
L_4 &= 0.30(13)(4) & L_8 &= 0.59(5)(2) \\
L_6 &= 0.24(10)(3) & \bar{\ell}_4 &= 4.01(16)(13) \\
\bar{\ell}_3 &= 3.15(64)(42) & \hat{m} &= 3.25(1)(7)(16)(0) \text{ MeV} \\
m_s &= 89.0(2)(16)(45)(1) \text{ MeV} & m_d &= 4.53(1)(8)(23)(12) \text{ MeV} \\
m_u &= 1.96(0)(6)(10)(12) \text{ MeV} & m_u/m_d &= 0.432(1)(9)(0)(39) . \\
m_s/\hat{m} &= 27.41(5)(22)(0)(4)
\end{aligned} \quad (2)$$

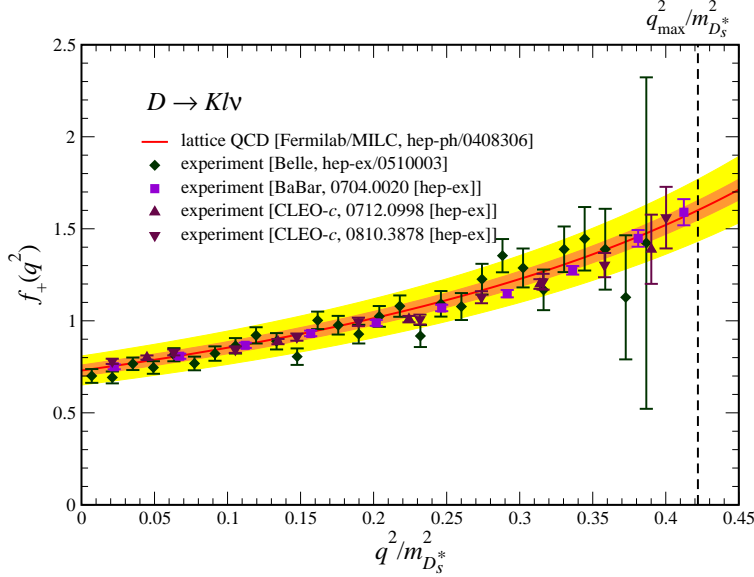


Figure 5: The semileptonic form factor $f_+(q^2)$ for the decay of a D meson into a K meson, a lepton, and a neutrino, as a function of the momentum transfer to the leptons q^2 . The orange curve is the lattice prediction and the plotting symbols are experimental results from the Belle, BaBar and CLEO-c collaborations.

The errors are statistical, lattice-systematic, perturbative (for masses and condensates; from two-loop perturbation theory [5]) and electromagnetic (for masses; from continuum estimates). f_2 (f_3) represents the three-flavor decay constant in the two (three) flavor chiral limit, and $\langle\bar{u}u\rangle_2$ ($\langle\bar{u}u\rangle_3$) is the corresponding condensate. The $SU(3)$ low energy constants L_i are in units of 10^{-3} and are evaluated at chiral scale m_η ; the $SU(2)$ low energy constants $\bar{\ell}_{3,4}$ are derived from the L_i and are scale invariant. The condensates and masses are in the $\overline{\text{MS}}$ scheme at scale 2 GeV.

Our result for m_u/m_d confirms, with improved control of the chiral extrapolations, our 2004 finding that ruled out the possibility that the (high-energy) up quark mass could vanish. This puts to rest a long standing proposal [6] that a vanishing up quark mass could solve the Strong CP Puzzle [7]. Alternative solutions are now more likely: *e. g.*, the axion [8], a possible component of Dark Matter.

The result for the CKM element $|V_{us}|$ comes, following Marciano [9], from our value of f_K/f_π and uses recent results for kaon leptonic branching fractions [4]. This result is competitive with the alternative determination $|V_{us}| = 0.2255(19)$ [4], which uses kaon semileptonic decays and continuum theory; an earlier version of our calculation has already been quoted by the Particle Data Group [4]. The determination of $|V_{us}|$ provides an important constraint on the Standard Model.

For comparison with Eq. 2, we give the results from the $SU(2)$ chiral fits for quantities involving only the u and d valence quarks:

$$\begin{aligned}
 f_2 &= 123.7(8)(14) \text{ MeV} & \langle\bar{u}u\rangle_2 &= -(280(3)(4)(4) \text{ MeV})^3 \\
 \bar{\ell}_3 &= 3.0(6)({}_{-6}^{+9}) & \bar{\ell}_4 &= 3.9(2)(3) \\
 \hat{m} &= 3.23(3)({}_{-3}^{+5})(16)(0) \text{ MeV} & &
 \end{aligned} \tag{3}$$

Weak decays of particles containing heavy quarks: We are engaged in a long term effort with the Fermilab Lattice Collaboration to study the decays and mixings of pseudoscalar mesons with one light and one heavy quark. Strong interaction effects in leptonic decays are characterized by decay constants, in semi-leptonic decays by various form factors, and in the mixing of neutral

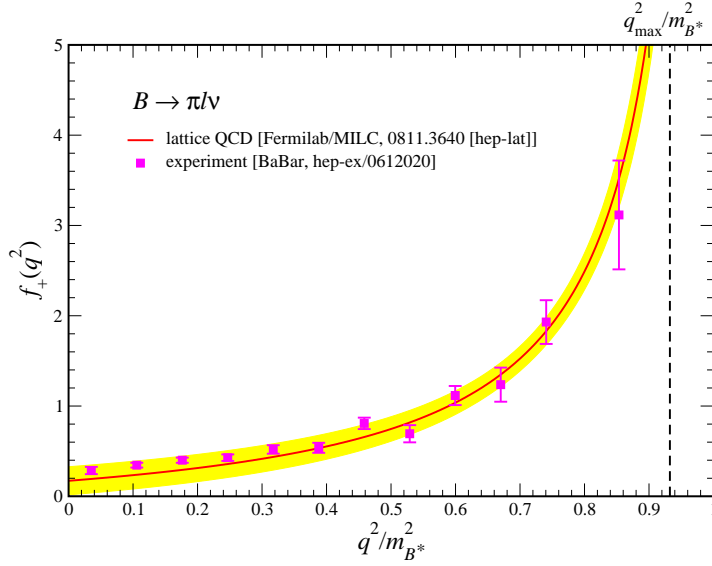


Figure 6: The form factor for the semileptonic decay $B \rightarrow \pi l \nu$. The solid line is the lattice predictions and the plotting symbols experimental results.

particles with their anti-particles by bag parameters. The values of these quantities for B and B_s mesons, which contain heavy b quarks, play a critical role in tests of the Standard Model that have been a major focus of the experimental program in high energy physics for a number of years. If the accuracy of lattice calculations can keep pace with the increasing accuracy of the related experiments, there will be important opportunities to sharpen tests of the Standard Model and search for new physics beyond it. At the same time, the decay constants and form factors of D and D_s mesons, which contain heavy c quarks, have been measured to high accuracy by the CLEO-c Collaboration and other experimental groups. Since the lattice techniques for studying mesons with c and b quarks are identical, these experiments provide an excellent opportunity to validate the lattice approach, as well as to make further tests of the Standard Model.

In 2005, we and our Fermilab collaborators predicted the leptonic decay constants of the D^+ and D_s mesons to be $f_{D^+} = 201 \pm 3 \pm 17$ MeV and $f_{D_s} = 249 \pm 3 \pm 15$ MeV, where the uncertainties are statistical and systematic [10]. Shortly thereafter, an experiment by the CLEO-c Collaboration found $f_{D^+} = 223 \pm 16_{-9}^{+7}$ MeV [11], and one by the BaBar Collaboration gave $f_{D_s} = 283 \pm 17 \pm 7 \pm 14$ MeV [12]. Thus, within statistical and systematic errors, there was agreement between the experimental results and lattice predictions. Over the last few years, however, both the experimental and lattice errors have been reduced significantly, and an interesting situation has emerged. The most recent results from the CLEO-c Collaboration are $f_{D^+} = 205.8 \pm 8.9$ MeV [13], and $f_{D_s} = 259.5 \pm 7.3$ MeV [14] and $f_{D^+}/f_{D_s} = 0.793 \pm 0.040$ [14]. We have improved the accuracy of our calculations by pushing to lattice spacings as small as $a \approx 0.09$ fm. Our current preliminary numbers are: $f_{D^+} = 207 \pm 11$ MeV, $f_{D_s} = 249 \pm 11$ MeV, and $f_{D^+}/f_{D_s} = 0.833 \pm 0.019$, in reasonable agreement with experiment. In the meantime, the HPQCD collaboration has published [15] the results for their lattice calculation using our Asqtad gauge configurations and highly improved staggered (HISQ) valence quark action [3]. They obtain $f_{D^+} = 207 \pm 4$ MeV, $f_{D_s} = 241 \pm 3$ MeV, and $f_{D^+}/f_{D_s} = 0.859 \pm 0.008$. So, while both lattice calculations for f_{D^+} are in agreement with experiment, there is a discrepancy between the HPQCD result for f_{D_s} and experiment. This discrepancy is even more marked for the ration f_{D^+}/f_{D_s} . Clearly, it is crucial to continue to improve the precision of the lattice determinations (as well as that of the experiments), and we are in the process of doing so.

In 2004, we and our Fermilab collaborators posted our initial results for the form factors of the

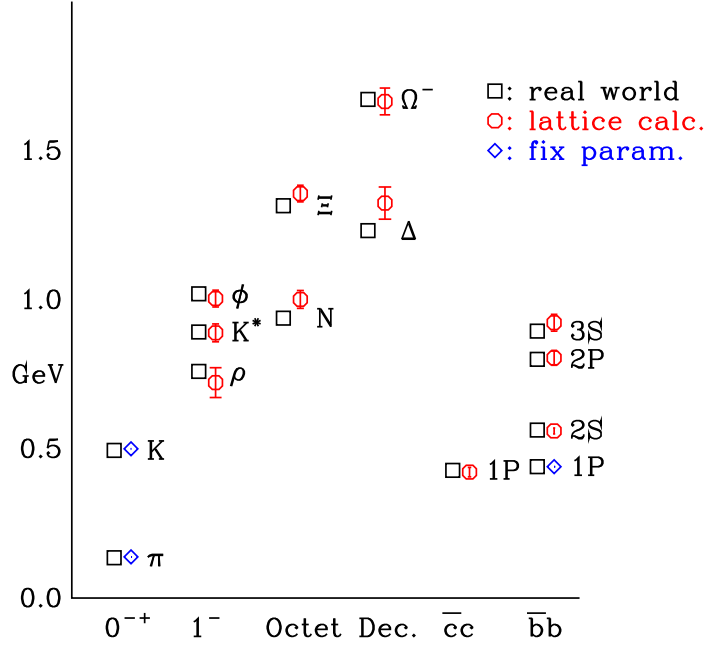


Figure 7: Comparison of lattice and experimental values for a variety of hadron masses and splittings.

semileptonic decay $D \rightarrow K\ell\nu$ [16]. Figure 5 compares our prediction with with data from a series of experiments giving progressively tighter confirmation of our result [17, 18, 19, 20]. More recently, we have carried out studies of other heavy-light quantities that are especially important in constraining the CKM matrix and searches for new physics. We have just completed calculations of the semileptonic form factors for the decays $B \rightarrow \pi\ell\nu$ [22] and $B \rightarrow D^*\ell\nu$ [23]. Figure 6 compares our result for the $B \rightarrow \pi\ell\nu$ form factor with an earlier experiment by the BaBar Collaboration [21]. The $B \rightarrow \pi\ell\nu$ form factor is used to extract $|V_{ub}|$, which provides a key constraint on the CKM matrix. The form factor must be calculated on the lattice at small pion recoil momentum, a region of phase space where, unfortunately, experimental errors are large. Analyticity and unitarity constraints are therefore used in a combined fit to lattice results and experimental data over a wide range of pion recoil momenta [24]. We obtained $|V_{ub}| = (3.38 \pm 0.36) \times 10^{-3}$, whereas the Particle Data Group gives $|V_{ub}| = (3.93 \pm 0.36) \times 10^{-3}$ from a world average dominated by inclusive measurements. The $B \rightarrow D^*\ell\nu$ form factor enables one to determine the CKM matrix element V_{cb} . Our result is $|V_{cb}| = (38.7 \pm 0.9 \pm 1.0) \times 10^{-3}$, where the first error is due to the experimental uncertainty in the $B \rightarrow D^*\ell\nu$ form factor, and the second is the lattice error. This result should be compared with the inclusive ($b \rightarrow c\ell\nu$) determination of $|V_{cb}| = (41.2 \pm 1.1) \times 10^{-3}$, which makes use of the operator product expansion and perturbation theory. We note that there is a slight discrepancy between the two determinations, and it is thus important to improve the lattice determination of this quantity.

The mass spectrum of strongly interacting particles: We are calculating the masses of strongly interacting particles as we generate gauge configurations [25]. With several quark masses and lattice spacings to work with, we can make extrapolations to the physical light quark mass and to the continuum limit. Figure 7 shows a comparison of several of the lightest hadrons with experiment, as well as splittings of $\bar{c}c$ and $\bar{b}b$ mesons calculated by the HPQCD and Fermilab Lattice Collaborations using our configurations. The known π and K masses are used to fix the light quark masses. The $\bar{c}c$ and $\bar{b}b$ (Υ) masses are shown as splittings relative to the $1S$ ground state. The Υ $1S - 1P$ splitting is used to determine the lattice spacing.

Strongly interacting matter under extreme conditions: We are currently seeking to significantly

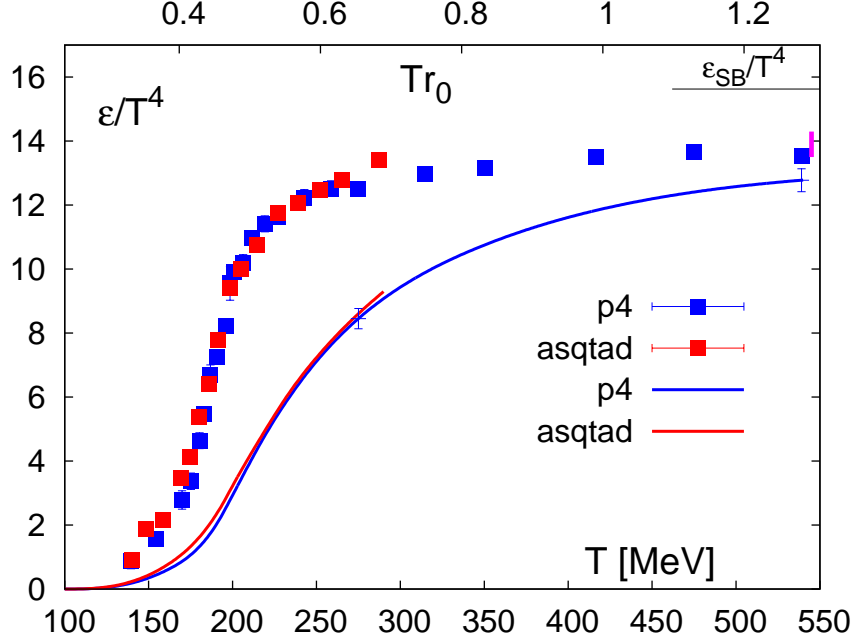


Figure 8: The energy density (squares) and pressure (solid curves) on lattices with eight time slices.

improve our determinations of the transition temperature and the equation of state through a new set of calculations on lattices with six and eight time slices. This project is being carried out as part of the work of the recently formed HotQCD Collaboration, of which we are members[26]. Figure 8 shows the energy density and three times the pressure as a function of temperature for the two different staggered actions being studied by the HotQCD Collaboration: Asqtad (red symbols) and Fat3p4 (blue symbols). Crosses with error bars indicate the systematic error in the pressure that arises from different integration schemes used to compute it. This quantity was calculated with an average light quark mass that is approximately twice as heavy as that in Nature. The excellent agreement between the two quark formulations, which have different finite lattice spacing artifacts, indicates that the results are close to those of the continuum. We estimate that lattice uncertainties that arise from finite lattice spacing and quark mass effects are of order 10%. An accurate determination of the equation of state is crucial to hydrodynamical modeling of the expansion and cooling of the quark-gluon plasma, and we present in Ref. [26] a parameterization of the equation of state suitable for input for hydrodynamic models of heavy ion collisions.

During the past year we have extended our study of the equation of state of the quark-gluon plasma for the Asqtad action by including the effects of the charm quark in the quenched approximation. That is, the charm quark appears as a valence quark, but not as a dynamical sea quark. Our results for the interaction measure, pressure and energy density with the addition of the charm quark are shown in Fig. 9 where we compare them to the data with three flavors of quark only. We conclude that the charm quark has a significant contribution to the equation of state at temperatures higher than about 225 MeV. It is an interesting observation that despite the largeness of the mass of the charm quark, its effects are pronounced and cannot be accounted for perturbatively. The equation of state with the charm quark added is most applicable to the study of the early universe, since the time scale relevant to the experimental conditions is too short for the charm quark to thermalize and have a visible effect on the particle data from the heavy-ion collisions. In addition, we have begun a study of the effects of the bottom quark on the quark-gluon plasma equation of state.

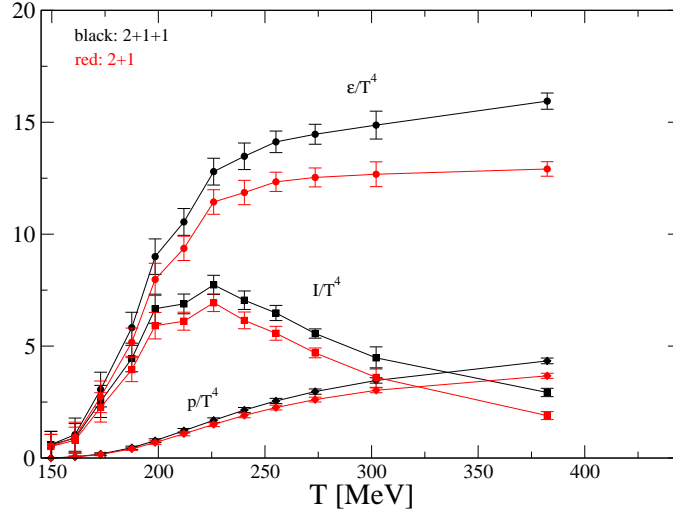


Figure 9: The interaction measure (I), pressure (p) and energy density (ϵ) of quark-gluon plasma with the charm quark added (black) compared with the case where we have only the up, down and strange quarks accounted for in our calculation (red).

References

- [1] The MILC Collaboration: C. Bernard *et al.*, Nucl. Phys. (Proc. Suppl.), **60A**, 297 (1998); Phys. Rev. D **58**, 014503 (1998); G.P. Lepage, Nucl. Phys. (Proc. Suppl.), **60A**, 267 (1998); Phys. Rev. D **59**, 074501 (1999); Kostas Orginos and Doug Toussaint (MILC), Nucl. Phys. (Proc. Suppl.), **73**, 909 (1999); Phys. Rev. D **59**, 014501 (1999); Kostas Orginos, Doug Toussaint and R.L. Sugar (MILC), Phys. Rev. D **60**, 054503 (1999); The MILC Collaboration: C. Bernard *et al.*, Phys. Rev. D **61**, 111502 (2000).
- [2] See, for example, J. Gasser and H. Leutwyler, Nucl. Phys. **B250**, 465 (1985).
- [3] The HPQCD/UKQCD Collaboration: E. Follana *et al.*, Phys. Rev. D **73**, 054502 (2007) [arXiv:hep-lat/0610092].
- [4] C. Amsler *et al.*, Physics Letters B667, 1 (2008) and 2009 partial update for the 2010 edition.
- [5] Q. Mason *et al.* [HPQCD Collaboration], Phys. Rev. D **73** (2006) 114501 [arXiv:hep-ph/0511160].
- [6] D. B. Kaplan and A. V. Manohar, Phys. Rev. Lett. **56**, 2004 (1986); A. G. Cohen, D. B. Kaplan and A. E. Nelson, JHEP **9911**, 027 (1999) [arXiv:hep-lat/9909091].
- [7] G. 't Hooft, Phys. Rev. Lett. **37**, 8 (1976), and Phys. Rev. D **14**, 3432 (1976); R. Jackiw and C. Rebbi, Phys. Rev. Lett. **37**, 172 (1976); C. Callan, R. Dashen, and D. Gross, Phys. Lett. **63B**, 334 (1976).
- [8] F. Wilczek, Phys. Rev. Lett. **40**, 279 (1978); R. Peccei and H. Quinn, Phys. Rev. Lett. **38**, 1440 (1978); S. Weinberg, Phys. Rev. Lett. **40**, 223 (1978); T. Goldman and C. Hoffman, Phys. Rev. Lett. **40**, 220 (1978).
- [9] W. J. Marciano, Phys. Rev. Lett. **93**, 231803 (2004) [arXiv:hep-ph/0402299].

- [10] The Fermilab Lattice, MILC and HPQCD Collaborations: C. Aubin *et al.*, Phys. Rev. Lett. **95** 122002 (2005).
- [11] The CLEO-c Collaboration: M. Artuso *et al.*, Phys. Rev. Lett. **95** 251801 (2005).
- [12] The BABAR Collaboration: B. Aubert *et al.*, Phys. Rev. Lett. **98**, 141801 (2007).
- [13] The CLEO-c Collaboration, B.I. Eisenstein, *et al*, Phys. Rev. **D78**, 052003 (2008) [arXiv:0806.2112].
- [14] The CLEO-c Collaboration, J.P. Alexander, *et al*, Phys. Rev. **D79**, 052001 (2009) [arXiv:0901.1216].
- [15] The HPQCD and UKQCD Collaborations: E. Follana, C. T. H. Davies, G. P. Lepage and J. Shigemitsu, Phys. Rev. Lett. **100**, 062002 (2008).
- [16] The Fermilab Lattice, MILC, and HPQCD/UKQCD Collaborations: C. Aubin *et al.*, Phys. Rev. Lett. **94**, 011601 (2005) [arXiv:hep-lat/0408306].
- [17] T. Lesiak, for the Belle Collaboration, AIP Conference Proceedings **814**, 493 (2006) [arXiv:hep-ex/0511003].
- [18] The BaBar Collaboration: B. Aubert *et al.*, arXiv:0704.0020 [hep-ex], submitted to Phys. Rev. D.
- [19] The CLEO-c Collaboration: D. Cronin-Hennessy *et al.*, Phys. Rev. Lett. **100**, 251801 (2008) [arXiv:0712.0998 hep-ex]].
- [20] The CLEO-c Collaboration: J. Ge *et al.*, arXiv:0810.3878 [hep-ex], submitted to Phys. Rev. D.
- [21] The BaBar Collaboration: B. Aubert *et al.*, Phys. Rev. Lett. **98**, 091801 (2007) [arXiv:hep-ex/0612020].
- [22] The Fermilab Lattice and MILC Collaborations: J. Bailey *et al.*, Phys. Rev. D **79**, 054507 (2009) [arXiv:0811.3640 [hep-lat]].
- [23] The Fermilab Lattice and MILC Collaborations: C. Bernard *et al.*, Phys. Rev. D **79**, 014506 (2009) [arXiv:0808.2519 [hep-lat]].
- [24] C. M. Arnesen, B. Grinstein, I. Rothstein, and I. Stewart, Phys. Rev. Lett. **95**, 071802 (2005).
- [25] The MILC Collaboration: C. Bernard *et al.*, Phys. Rev. **D64**, 054506(2001); Phys. Rev. **D70**, 094505 (2004).
- [26] The HotQCD Collaboration: A. Bazavov, *et al.*, arXiv:0903.4379 [hep-lat], to be published in Phys. Rev. D.